Factorization and high-energy effective action

Ian Balitsky*
Physics Department, Old Dominion University, Norfolk, Virginia 23529
and Theory Group, Jefferson Lab, Newport News, Virginia 23606
(Received 10 December 1998; published 14 June 1999)

I demonstrate that the amplitude for high-energy scattering can be factorized as a convolution of the contributions due to fast and slow fields. The fast and slow fields interact by means of Wilson-line operators—infinite gauge factors ordered along the straight line. The resulting factorization formula gives a starting point for a new approach to the effective action for high-energy scattering in QCD. [S0556-2821(99)03413-X]

PACS number(s): 12.38.Bx, 11.10.Jj, 11.55.Jy

I. INTRODUCTION

In the leading logarithmic approximation, the high-energy scattering in perturbative QCD is determined by the Balitsky-Fadin-Kuraev-Lipatov (BFKL) Pomeron [1]. It is well known that the power behavior of BFKL cross section violates the Froissart bound. The BFKL Pomeron describes only the pre-asymptotic behavior at not very large energies and in order to find the true high-energy asymptotics in perturbative QCD we need to unitarize the BFKL Pomeron. This is a difficult problem which has been in need of a solution for more than 20 years. However, until recently, it was a common belief that at least at present energies (e.g. for small-x deep inelastic scattering at the DESY ep collider HERA) the corrections to BFKL Pomeron are small so they can be neglected. Contrary to those expectations, recent calculation of the next-to-leading correction to the BFKL kernel [2] shows that this correction is very big. It is very likely that further corrections are also large which means that we must deal with the problem of the unitarization of the BFKL Pomeron at present energies.

One of the most popular ideas in solving this problem is to reduce the QCD at high energies to some sort of two-dimensional effective theory which will be simpler than the original QCD, maybe even to the extent of exact solvability. Some attempts in this direction were made starting from the work [3], but the matter is an open issue for the time being. In this paper I will describe a new approach to the effective action which is based on factorization in rapidity space for high-energy scattering.

The form of factorization is dictated by process kinematics (for a review, see [4]). A classical example is the factorization of the structure functions of deep inelastic scattering into coefficient functions and parton densities. In the case of deep inelastic scattering, there are two different scales of transverse momentum and it is therefore natural to factorize the amplitude in the product of contributions of hard and soft parts coming from the regions of small and large transverse momenta, respectively. On the contrary, in the case of high-energy (Regge-type) processes, all the transverse momenta are of the same order of magnitude, but colliding particles strongly differ in rapidity so it is natural to factorize in the rapidity space.

Factorization in rapidity space means that the high-energy scattering amplitude can be represented as a convolution of contributions due to ''fast'' and ''slow'' fields. To be precise, we choose a certain rapidity η_0 to be a ''rapidity divide'' and we call fields with $\eta > \eta_0$ fast and fields with $\eta < \eta_0$ slow where η_0 lies in the region between spectator rapidity η_A and target rapidity η_B. (The interpretation of these fields as fast and slow is literally true only in the rest frame of the target but we will use this terminology for any frame.)

To explain what we mean by the factorization in rapidity space let us recall the operator expansion for high-energy scattering [5] where the explicit integration over fast fields gives the coefficient functions for the Wilson-line operators representing the integrals over slow fields. For a $2\Rightarrow 2$ particle scattering in Regge limit $s \gg m^2$ [where m is a common mass scale for all other momenta in the problem $t \sim p_A^2 \sim (p_A')^2 \sim p_B^2 \sim (p_B')^2 \sim m^2$] we have

$$A(p_A, p_B \Rightarrow p_A', p_B') = \sum \int d^2x_1 \ldots d^2x_n C^{i_1 \ldots i_n}(x_1, \ldots x_n) \langle p_B | \mathrm{Tr}\{U_{i_1}(x_1) \ldots U_{i_n}(x_n)\} | p_B' \rangle. \quad (1)$$

[As usual, $s=(p_A+p_B)^2$ and $t=(p_A-p_A')^2$.] Here $x_i (i=1,2)$ are the transverse coordinates (orthogonal to both p_A and p_B) and $U_i(x) = U^\dagger(x)(i/g)(\partial/\partial x_i)U(x)$ where the Wilson-line operator $U(x)$ is the gauge link ordered along the infinite straight line corresponding to the ''rapidity divide'' η_0. Both coefficient functions and matrix elements in Eq. (1) depend on the η_0 but this dependence is canceled in

*Email address: balitsky@jlab.org

the physical amplitude just as the scale μ (separating coefficient functions and matrix elements) disappears from the final results for structure functions in case of usual factorization. Typically, we have the factors $\sim(g^2\ln s/m^2-\eta_0)$ coming from the ''fast'' integral and the factors $\sim g^2\eta_0$ coming from the ''slow'' integral so they combine in a usual log factor $g^2\ln s/m^2$. In the leading log approximation these factors sum up into the BFKL Pomeron (for a review see Ref. [6]).

Unlike usual factorization, the expansion (1) does not have the additional meaning of perturbative vs nonperturbative separation—both the coefficient functions and the matrix elements have perturbative and nonperturbative parts. This happens due to the fact that the coupling constant in a scattering process is determined by the scale of transverse momenta. When we perform the usual factorization in hard ($k_\perp>\mu$) and soft ($k_\perp<\mu$) momenta, we calculate the coefficient functions perturbatively [because $\alpha_s(k_\perp>\mu)$ is small] whereas the matrix elements are nonperturbative. Conversely, when we factorize the amplitude in rapidity, both fast and slow parts have contributions coming from the regions of large and small $k_\perp$. In this sense, coefficient functions and matrix elements enter the expansion (1) on equal footing. We could have integrated first over slow fields (having the rapidities close to that of p_B) and the expansion would have the form

$$A(s,t)=\sum\int d^2x_1\ldots d^2x_n D^{i_1\cdots i_n}(x_1,\ldots x_n)\langle p_A|\mathrm{Tr}\{U_{i_1}(x_1)\ldots U_{i_n}(x_n)\}|p_A'\rangle. \tag{2}$$

In this case, the coefficient functions D are the results of integration over slow fields and the matrix elements of the U operators contain only the large rapidities $\eta>\eta_0$. The symmetry between Eqs. (1) and (2) calls for a factorization formula which would have this symmetry between slow and fast fields in explicit form.

I will demonstrate that one can combine the operator expansions (1) and (2) in the following way:

$$A(s,t)=\sum\frac{i^n}{n!}\int d^2x_1\ldots d^2x_n\langle p_A|U^{a_1i_1}(x_1)\ldots U^{a_ni_n}(x_n)|p_A'\rangle\langle p_B|U^{a_1}_{i_1}(x_1)\ldots U^{a_n}_{i_n}(x_n)|p_B'\rangle, \tag{3}$$

where $U_i^a\equiv\mathrm{Tr}(\lambda^a U_i)$ (λ^a are the Gell-Mann matrices). It is possible to rewrite this factorization formula in a more visual form if we agree that operators U act only on states B and B' and introduce the notation V_i for the same operator as U_i only acting on the A and A' states:

$$A(s,t)=\langle p_A|\langle p_B|\exp\left(i\int d^2xV^{ai}(x)U_i^a(x)\right)|p_A'\rangle|p_B'\rangle. \tag{4}$$

In a sense, this formula amounts to writing the coefficient functions in Eq. (1) [or Eq. (2)] as matrix elements of Wilson-line operators. Equation (4) illustrated in Fig. 1 is our main tool for factorizing in rapidity space.

In order to define an effective action for a given interval in rapidity $\eta_0>\eta>\eta_0'$ we use the master formula (4) two times as illustrated in Fig. 2. We obtain then

$$A(s,t)=\langle p_A|\langle p_B|e^{iS_{\mathrm{eff}}(V_i,Y_j)}|p_A'\rangle|p_B'\rangle, \tag{5}$$

where the Wilson-line operators $Y_i(x_\perp)$ have the same form as $U_i(x_\perp)$ but aligned along the n' direction [and act only on B and B' states, cf. Eq. (4)]. In this formula, the region of rapidities greater than η_0 is represented by operators V_i acting on the spectator A and A' states, the region of rapidities lower than η_0' by the operators Y_i acting on target B and B' states, and the region $\eta_0>\eta>\eta_0'$ is integrated out—all the information about it is contained in the effective action $S_{\mathrm{eff}}(V_i,Y_j)$. As we shall see below, this effective action is in general nonlocal [unlike the local interaction term $\int dx_\perp V_i(x_\perp)U_i(x_\perp)$ in the factorization formula (4)]. Moreover, it contains the factors $g^2(\eta_0-\eta_0')$ which are the usual high-energy logarithms $g^2\ln(s_0/s_0')$ where the energies s_0 and s_0' correspond to rapidities η_0 and η_0'. If we had a complete expression for $S_{\mathrm{eff}}(\eta_0,\eta_0')$ we could take $\eta_0=\eta_A$ (rapidity of the spectator particle) and $\eta_0'=\eta_B$ (rapidity of the target

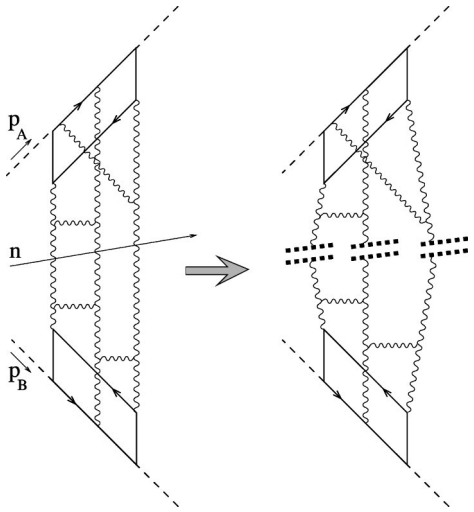

FIG. 1. Structure of the factorization formula. Dashed, solid, and wavy lines denote photons, quarks, and gluons, respectively. Wilson-line operators are denoted by dotted lines and the vector n gives the direction of the ''rapidity divide'' between fast and slow fields.

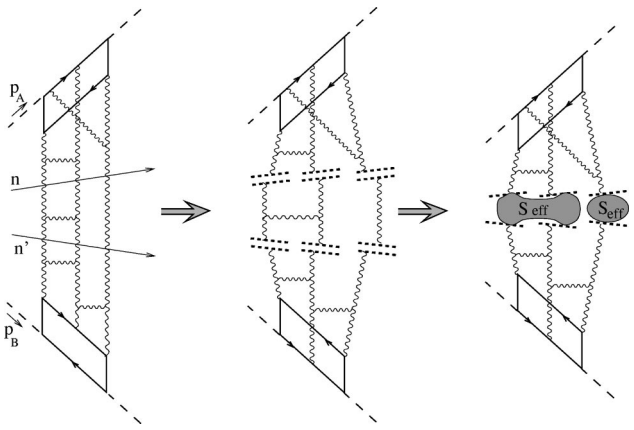

FIG. 2. The effective action for the interval of rapidities $\eta_0 > \eta > \eta_0'$. The two vectors n and n' correspond to ''rapidity divides'' η_0 and η_0' bordering our chosen region of rapidities.

particle), then all the logarithmic dependence on the energy would be included in the effective action and the resulting matrix elements of the operators V_i between A states and operators Y between B states will contain no logarithms (and may be calculated in the first order in perturbation theory for suitable A and B particles such as virtual photons). Since multiple rescatterings are taken into account by $e^{iS_{\rm eff}}$ automatically the corresponding amplitude must be unitary. This program is probably not less difficult than the direct calculation of the many-Pomeron exchanges in the perturbation theory but for the case of effective-action language we have some additional powerful methods such as semiclassical approach.

The paper is organized as follows. In Sec. II we recall the Wilson-line operator language for small-x physics. The factorization formula (4) is derived in Sec. III and in Sec. IV we use it to define formally the high-energy effective action for a given interval in rapidity (some of the results of this section were reported earlier in the Letter [7]). A semiclassical approach to calculation of this effective action is discussed in Sec. V and Sec. VI contains conclusions and outlook.

II. OPERATOR EXPANSION FOR HIGH-ENERGY SCATTERING

Let us now briefly recall how to obtain the operator expansion (1). For simplicity, consider the classical example of high-energy scattering of virtual photons with virtualities $\sim -m^2$:

$$A(s,t) = -i\langle 0|T\{j(p_A)j(p_A')j(p_B)j(p_B')\}|0\rangle, \qquad (6)$$

where $j(p)$ is the Fourier transform of electromagnetic current $j_\mu(x)$ multiplied by some suitable polarization $e^\mu(p)$. At high energies it is convenient to use the Sudakov decomposition:

$$p^\mu = \alpha_p p_1^\mu + \beta_p p_2^\mu + p_\perp^\mu \qquad (7)$$

where p_1^μ and p_2^μ are the light-like vectors close to p_A and p_B, respectively $(p_A^\mu = p_1^\mu - p_2^\mu p_A^2/s,\ p_B^\mu = p_2^\mu - p_1^\mu p_B^2/s)$.

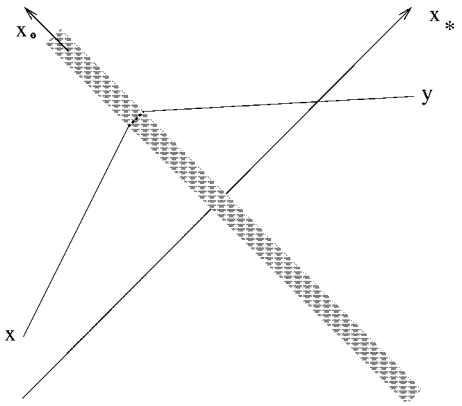

FIG. 3. Quark propagator in a shock-wave background.

We want to integrate over the fields with $\alpha > \sigma$ where σ is defined in such a way that the corresponding rapidity is η_0. [In explicit form $\eta_0 = \ln(\sigma/\tilde{\sigma})$ where $\tilde{\sigma} \equiv (m^2/s\sigma)$.] The result of the integration will be given by Green functions of the fast particles in slow ''external'' fields [5] (see also Ref. [8]). Since the fast particle moves along a straight-line classical trajectory the propagator is proportional to the straight-line ordered gauge factor U [9]. For example, when $x_+ > 0$, $y_+ < 0$ it has the form [5]

$$G(x,y) = i\int dz\,\delta(z_*)\frac{(\not{x}-\not{z})\not{p}_2}{2\pi^2(x-z)^4}U(z_\perp)\frac{\not{z}-\not{y}}{2\pi^2(z-y)^4}. \qquad (8)$$

We use the notations $z_\cdot \equiv z_\mu p_1^\mu$ and $z_* \equiv z_\mu p_2^\mu$ which are essentially identical to the light-front coordinates: $z_* = z_+\sqrt{s/2}$, $z_\cdot = z_-\sqrt{s/2}$ [where $z_\pm = (1/\sqrt{2})(z^0 \pm z^3)$]. The Wilson-line operator U is defined as follows:

$$U(x_\perp) = [\infty p_1 + x_\perp, -\infty p_1 + x_\perp], \qquad (9)$$

where $[x,y]$ is the straight-line ordered gauge link suspended between the points x and y:

$$[x,y] \stackrel{\rm def}{\equiv} P\exp\left(ig\int_0^1 du(x-y)^\mu A_\mu[ux+(1-u)y]\right). \qquad (10)$$

The origin of Eq. (3) is more clear in the rest frame of the ''A'' photon (see Fig. 3). Then the quark is slow and the external fields are approaching this quark at high speed. Due to the Lorentz contraction, these fields are squeezed in a shock wave located at $z_* = 0$ (in a suitable gauge like the Feynman one). Therefore, the propagator (8) of the quark in this shock-wave background is a product of three factors which reflect (i) free propagation from x to the shock wave, (ii) instantaneous interaction with the shock wave which is described by the operator[1] $U(z_\perp)$, and (iii) free propagation from the point of interaction z to the final destination y.

[1]Because the shock wave is very thin, the quark has no time to deviate in the transverse direction. Therefore the quark's trajectory

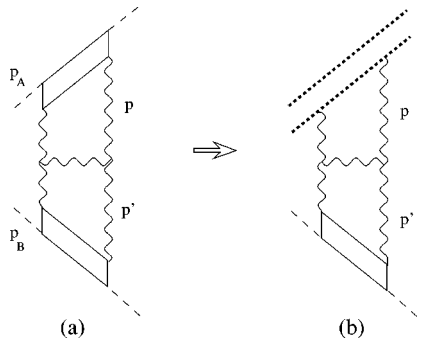

FIG. 4. A typical Feynman diagram for the $\gamma^*\gamma^*$ scattering amplitude (a) and the corresponding two-Wilson-line operator (b).

The propagation of the quark-antiquark pair in the shock-wave background is described by the product of two propagators of Eq. (8) type which contain two Wilson-line factors $U(z)U^\dagger(z')$, where z' is the point where the antiquark crosses the shock wave. If we substitute this quark-antiquark propagator in the original expression for the amplitude (6) we obtain [5]

$$\int d^4x d^4z e^{ip_A\cdot x+iq\cdot z}\langle T\{j(x+z)j(z)\}\rangle_A$$

$$\simeq \int \frac{d^2p_\perp}{4\pi^2} I(p_\perp,q_\perp)\mathrm{Tr}\{U(p_\perp)U^\dagger(q_\perp-p_\perp)\}, \quad (11)$$

where $U(p_\perp)$ is the Fourier transform of $U(x_\perp)$ and $I(p_\perp,q_\perp)$ is the so-called ''impact factor'' which is a function of $p_\perp^2, p_\perp\cdot q_\perp$, and photon virtuality [10,5]. Thus, we have reproduced the leading term in the expansion (1). [To recognize it, note that

$$U^\dagger(x_\perp)U(y_\perp)=P\exp\{-ig\textstyle\int_y^x dz_i U_i(z_\perp)\}$$

where the precise form of the path between points $x_\perp$ and $y_\perp$ does not matter since this is actually a formula for the gauge link in a pure gauge field $U_i(z_\perp)$]. So, in the leading order in perturbation theory we have calculated the integral over fast fields explicitly and reduced the remaining integral over slow fields to the matrix element of the two-Wilson-line operator; see Fig. 4. It is worth noting that in the next order in perturbation theory we will get the contribution to the right-hand side of Eq. (11) proportional to four-Wilson-line operators, in the next to six-line operators and so on.

Note that formally we have obtained the operators U ordered along the light-like lines. Matrix elements of such operators contain divergent longitudinal integrations which reflect the fact that the light-like gauge factor corresponds to a quark moving with the speed of light (i.e., with infinite energy). This divergency can be seen already at the one-loop level if one calculates the contribution to the matrix element of the two-Wilson-line operator $U(x_\perp)U^\dagger(y_\perp)$ between the ''virtual photon states'' shown in Fig. 4. The reason for this divergency is very simple. We have replaced the fast-quark propagator in the ''external field'' (represented here by two gluons coming from the bottom part of the diagram) by the light-like Wilson line. In doing so we have assumed that these two gluons are slow, $\eta_p \ll \eta_A$. However, when we calculate the matrix element of the $U(x_\perp)U^\dagger(y_\perp)$ formally the integration over the rapidities of the gluon η_p is unbounded so our divergency comes from the fast part of the external field which really does not belong there. Indeed, if the rapidity of the gluon η_p is of the order of the rapidity of the quark this gluon is a fast one so it will contribute to the coefficient function (in front of the operator constructed from the slow fields) rather than to the matrix element of the operator.

This is very similar to the case of usual light-cone expansion for the deep inelastic scattering (DIS) at moderate x. In that case, we at first expand near the light cone (in inverse powers of Q^2). The result is that the amplitude of DIS is reduced to matrix elements of the light-cone operators which are known as parton densities in the nucleon. These matrix elements contain logarithmical divergence in transverse momenta for the same reason as above—when expanding around the light cone we assumed that there are no hard quarks and gluons inside the proton, but matrix elements of light-cone operators contain formally unbounded integrations over $k_\perp^2$. It is well known how to proceed in this case: we define the renormalized light-cone operators with the transverse momenta $k_\perp^2>\mu^2$ cut off and expand our T-product of electromagnetic currents in a set of these renormalized light-cone operators rather than in a set of the original unrenormalized ones (see, e.g., [11]). After that, the matrix elements of these operators (parton densities) contain factors $\ln(\mu^2/m^2)$ and the corresponding coefficient functions contain $\ln(Q^2/\mu^2)$. When we calculate the amplitude we add these factors together so the dependence on the factorization scale μ cancels and we get the usual deep inelastic scattering (DIS) logarithmical factors $\ln(Q^2/m^2)$.

Similarly, we need some regularization of the Wilson-line operator which cuts off the fast gluons. As demonstrated in [5], it can be done by changing the slope of the supporting line. If we wish the longitudinal integration stop at $\eta=\eta_0$, we should order our gauge factors U along a line parallel to $n=\sigma p_1+\tilde{\sigma}p_2$, then the coefficient functions in front of Wilson-line operators (impact factors) will contain logarithms $\sim g^2\ln 1/\sigma$. Similarly to DIS, when we calculate the amplitude, we add the terms $\sim g^2\ln 1/\sigma$ coming from the coefficient functions (see Fig. 5b) to the terms $\sim g^2\ln[(\sigma/m^2/s)]$ coming from matrix elements (see Fig. 5a) so that the dependence on the ''rapidity divide'' σ cancels and we get the usual high-energy factors $g^2\ln(s/m^2)$ which are responsible for BFKL Pomeron.

inside the shock wave can be approximated by a light-like straight line, which means that the interaction of the quark with the shock wave will be described by a gauge factor ordered along this segment of a straight line. Since there is no field outside the shock-wave ''wall'' one can formally extend the limits of integration in a gauge factor to $\pm\infty$ which gives the operator U.

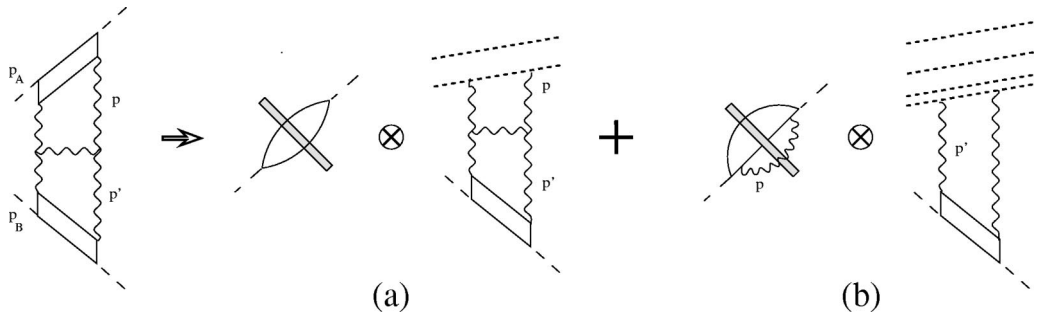

FIG. 5. Decomposition into product of coefficient function and matrix element of the two-Wilson-line operator for a typical Feynman diagram. (Double Wilson line corresponds to fast-moving gluon.)

III. FACTORIZATION FORMULA FOR HIGH-ENERGY SCATTERING

In order to understand how this expansion can be generated by the factorization formula of Eq. (3) type we have to rederive the operator expansion in axial gauge $A_\cdot=0$ with an additional condition $A_*|_{x_*=-\infty}=0$ (the existence of such a gauge was illustrated in [12] by an explicit construction). It is important to note that with power accuracy (up to corrections $\sim\sigma$) our gauge condition may be replaced by $n^\mu A_\mu=0$. In this gauge the coefficient functions are given by Feynman diagrams in the external field

$$B_i(x)=U_i(x_\perp)\Theta(x_*),\quad B_\cdot=B_*=0 \tag{12}$$

which is a gauge rotation of our shock wave [it is easy to see that the only nonzero component of the field strength tensor $F_{\cdot i}(x)=U_i(x_\perp)\delta(x_*)$ corresponds to shock wave]. The Green functions in external field (12) can be obtained from a generating functional with a source responsible for this external field. Normally, the source for given external field $\bar{\mathcal{A}}_\mu$ is just $J_\nu=\bar{D}^\mu\bar{F}_{\mu\nu}$ so in our case the only nonvanishing contribution is $J_\cdot(B)=\bar{D}^i\bar{F}_{i\cdot}$. However, we have a problem because the field which we try to create by this source does not decrease at infinity. To illustrate the problem, suppose that we use another light-like gauge $\mathcal{A}_*=0$ for a calculation of the propagators in the external field (12). In this case, the only would-be nonzero contribution to the source term in the functional integral $\bar{D}^i\bar{F}_{i\cdot}\mathcal{A}_*$ vanishes, and it looks like we do not need a source at all to generate the field B_μ. (This is of course wrong since B_μ is not a classical solution.) What it really means is that the source in this case lies entirely at infinity. Indeed, when we are trying to make an external field $\bar{\mathcal{A}}$ in the functional integral by the source J_μ we need to make a shift $\mathcal{A}_\mu\to\mathcal{A}_\mu+\bar{\mathcal{A}}_\mu$ in the functional integral

$$\int \mathcal{D}\mathcal{A}\exp\left\{iS(\mathcal{A})-i\int d^4x J^a_\mu(x)\mathcal{A}^{a\mu}(x)\right\}, \tag{13}$$

after which the linear term $\bar{D}^\mu\bar{F}_{\mu\nu}\mathcal{A}^\nu$ cancels with our source term $J_\mu\mathcal{A}^\mu$ and the terms quadratic in $\mathcal{A}$ make the Green functions in the external field $\bar{\mathcal{A}}$. [Note that the classical action $S(\bar{\mathcal{A}})$ for our external field $\bar{\mathcal{A}}=B$ (12) vanishes.] However, in order to reduce the linear term $\int d^4x\bar{F}^{\mu\nu}\bar{D}_\mu\mathcal{A}_\nu$ in the functional integral to the form $\int d^4x\bar{D}^\mu\bar{F}_{\mu\nu}\mathcal{A}^\nu(x)$ we need to make an integration by parts, and if the external field does not decrease there will be additional surface terms at infinity. In our case we are trying to make the external field $\bar{\mathcal{A}}=B$ so the linear term which needs to be canceled by the source is

$$\frac{2}{s}\int dx_\cdot dx_* d^2x_\perp \bar{F}_{i\cdot}\bar{D}_*\mathcal{A}^i=\int dx_* d^2x_\perp \bar{F}_{i\cdot}\mathcal{A}^i\Big|^{x_\cdot=\infty}_{x_\cdot=-\infty}. \tag{14}$$

It comes entirely from the boundaries of integration. If we recall that in our case $\bar{F}_{\cdot i}(x)=U_i(x_\perp)\delta(x_*)$ we can finally rewrite the linear term as

$$\int d^2x_\perp U_i(x_\perp)\{\mathcal{A}^i(-\infty p_2+x_\perp)-\mathcal{A}^i(\infty p_2+x_\perp)\}. \tag{15}$$

The source term which we must add to the exponent in the functional integral to cancel the linear term after the shift is given by Eq. (15) with the minus sign. Thus, Feynman diagrams in the external field (12) in the light-like gauge $\mathcal{A}_*=0$ are generated by the functional integral

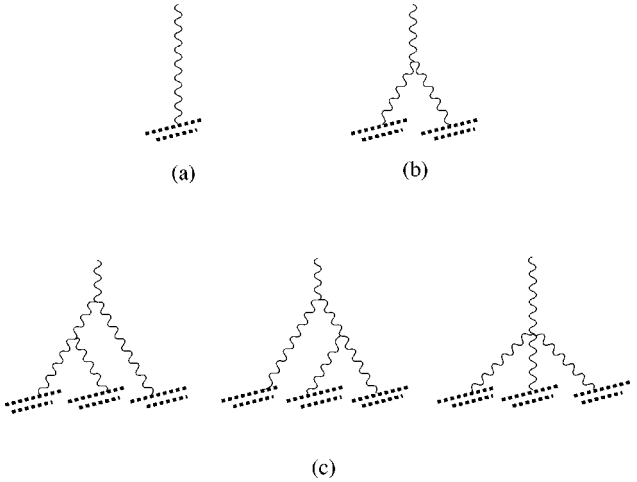

FIG. 6. Perturbative diagrams for the classical field (12).

$$\int \mathcal{D}\mathcal{A}\exp\left\{iS(\mathcal{A})+i\int d^2x_\perp U^{ai}(x_\perp)[\mathcal{A}_i^a(\infty p_2+x_\perp)-\mathcal{A}^{ai}(-\infty p_2+x_\perp)]\right\}. \tag{16}$$

In an arbitrary gauge the source term in the exponent in Eq. (16) can be rewritten in the form

$$2i\int d^2x_\perp \mathrm{Tr}\left\{U^i(x_\perp)\int_{-\infty}^{\infty}dv[-\infty p_2,vp_2]_{x_\perp}F_{*i}(vp_2+x_\perp)[vp_2,-\infty p_2]_{x_\perp}\right\}. \tag{17}$$

(Hereafter we use the space-saving notation $[up_2,vp_2]_{x_\perp}\equiv[up_2+x_\perp,vp_2+x_\perp]$ and similar notation for gauge link ordered along p_1.) Thus, we have found the generating functional for our Feynman diagrams in the external field (13).

It is instructive to see how the source (17) creates the field (12) in perturbation theory. To this end, we must calculate the field

$$\overline{\mathcal{A}}_\mu(x)=\int \mathcal{D}\mathcal{A}\mathcal{A}_\mu(x)\exp\left\{iS(\mathcal{A})+2i\int d^2x_\perp \mathrm{Tr}\left\{U^i(x_\perp)\int_{-\infty}^{\infty}dv[-\infty p_2,vp_2]_{x_\perp}F_{*i}(vp_2+x_\perp)[vp_2,-\infty p_2]_{x_\perp}\right\}\right\} \tag{18}$$

by expansion of both $S(\mathcal{A})$ and gauge links in the source term (17) in powers of g (see Fig. 6). In the first order one gets

$$\overline{\mathcal{A}}_\mu^{(0)}(x)=\int_{-\infty}^{\infty}dv\int dz_\perp U^{ia}(z_\perp)\langle\mathcal{A}_\mu(x)F^a_{*i}(vp_2+z_\perp)\rangle \tag{19}$$

where $\langle\mathcal{O}\rangle\equiv\int\mathcal{D}\mathcal{A}e^{iS_0}\mathcal{O}$. Now we must choose a proper gauge for our calculation. We are trying to create a field (12) perturbatively and therefore the gauge for our perturbative calculation must be compatible with the form (12) — otherwise, we will end up with the gauge rotation of the field $B(x)$. [For example, in Feynman gauge we will get the field $\overline{\mathcal{A}}_\mu$ of the form of the shock wave $\overline{\mathcal{A}}_i=\overline{\mathcal{A}}_*=0$, $\overline{\mathcal{A}}_\cdot\sim\delta(x_*)$.] It is convenient to choose the temporal gauge[2] $\mathcal{A}_0=0$ with the boundary condition $\mathcal{A}|_{t=-\infty}=0$ where

$$\mathcal{A}_\mu(t,\vec{x})=\int_{-\infty}^{t}dt'F_{0\mu}(t',\vec{x}). \tag{20}$$

In this gauge we obtain

$$\overline{\mathcal{A}}_\mu^{(0)}(x)=\int\frac{dp}{(2\pi)^3}\left(g_{\mu\nu}-2\frac{p_\mu(p_1+p_2)_\nu+(\mu\leftrightarrow\nu)}{s(\alpha+\beta+i\epsilon)}+\frac{4p_\mu p_\nu}{s^2(\alpha+\beta+i\epsilon)^2}\right)\frac{1}{\alpha\beta s-p_\perp^2+i\epsilon}$$
$$\times\int dz_\perp e^{i\alpha x_\cdot+i\beta x_*-i\vec{p}_\perp(\vec{x}-\vec{z})_\perp}p_{2\nu}\delta\left(\alpha\frac{s}{2}\right)\partial_i U^{ia}(z_\perp) \tag{21}$$

where $\delta(\alpha s/2)$ comes from the $\int dv e^{iv\alpha(s/2)}$. [Note that the form of the singularity $1/(p_0+i\epsilon)$ which follows from Eq. (20) differs from conventional Mandelstam-Leibbrandt prescription $V.p.(1/p_0)$.] Recalling that in terms of Sudakov variables $dp=(s/2)d\alpha d\beta dp_\perp$ one easily gets that $\overline{\mathcal{A}}_*^{(0)}=\overline{\mathcal{A}}_\cdot^{(0)}=0$ and

$$\overline{\mathcal{A}}_i^{(0)}(x)=\theta(x_*)\int\frac{dp}{(2\pi)^2}\frac{1}{p_\perp^2}\int dz_\perp e^{-i\vec{p}_\perp(\vec{x}-\vec{z})_\perp}\partial_i\partial_j U^{ja}(z_\perp), \tag{22}$$

which can be written down formally as

$$-\theta(x_*)\frac{1}{\partial_\perp^2}\partial_i\partial_j U^j(x_\perp)=U_i(x_\perp)\theta(x_*)-\theta(x_*)\frac{1}{\partial_\perp^2}(\partial_\perp^2 g_{ij}+\partial_i\partial_j)U^j(x_\perp) \tag{23}$$

[2]The gauge $\mathcal{A}_*=0$ which we used above is too singular for the perturbative calculation. In this gauge one must first regulate the external field (12) by, say, replacement $U_i\theta(x_*)\to U_i\theta(x_*)e^{-\epsilon x_\cdot}$ and let $\epsilon\to 0$ only in the final results.

(in our notations $\partial_\perp^2 \equiv -\partial_i\partial^i$). Now, since $U_i(x)$ is a pure gauge field (with respect to transverse coordinates) we have $\partial_i U_j - \partial_j U_i = i[U_i, U_j]$ so

$$\overline{\mathcal{A}}_i^{(0)}(x) = U_i(x_\perp)\,\theta(x_*) - \theta(x_*) ig \frac{\partial_j}{\partial_\perp^2}[U_i, U_j](x_\perp). \tag{24}$$

Thus, we have reproduced the field (12) up to the correction of g. We will demonstrate now that this $O(g)$ correction is canceled by the next-to-leading term in the expansion of the exponent of the source term in Eq. (18). In the next-to-leading order one gets (see Fig. 6b)

$$\overline{\mathcal{A}}_\mu^{(1)}(x) = g\int dy \int dz_\perp dz'_\perp U^{ja}(z_\perp) U^{kb}(z'_\perp) \times \left\langle \mathcal{A}_\mu(x) 2\mathrm{Tr}\{\partial_\alpha \mathcal{A}_\beta(y)[\mathcal{A}_\alpha(y), \mathcal{A}_\beta(y)]\} \int dv F^a_{*j}(v p_2 + z_\perp) \int dv' F^b_{*k}(v p_2 + z'_\perp) \right\rangle. \tag{25}$$

It is easy to see that $\overline{\mathcal{A}}_*^{(1)} = \overline{\mathcal{A}}_\cdot^{(1)} = 0$ and

$$\overline{\mathcal{A}}_i^{(1)}(x) = g\int dy \int \frac{dp}{(2\pi)^4 i} e^{-ip(x-y)} \frac{1}{p^2} (\partial^k [\mathcal{A}_i^{(0)}(y), \mathcal{A}_k^{(0)}(y)] + [\mathcal{A}^{(0)k}(y), \partial_i \mathcal{A}_k^{(0)}(y) - (i \leftrightarrow k)]). \tag{26}$$

Since $\mathcal{A}_k^{(0)}$ is given by Eq. (24) this reduces to

$$\overline{\mathcal{A}}_i^{(1)}(x) = -g\,\theta(x_*) \int dy_\perp \frac{dp_\perp}{(2\pi)^2} \frac{e^{-ip_\perp (x-y)_\perp}}{p_\perp^2} i\partial^k([U_i(y), U_k(y)]) + O(g^2) \tag{27}$$

which cancels the second term in Eq. (24). Thus, we obtain

$$\overline{\mathcal{A}}_i(x) = U_i(x_\perp)\,\theta(x_*) + O(g^2). \tag{28}$$

Similarly, one can check that the contributions $\sim g^2$ coming from the diagrams in Fig. 6c cancel the g^2 term in Eq. (28) and so on, leading finally to the expression $U_i(x_\perp)\,\theta(x_*)$ without any corrections.

We have found the generating functional for the diagrams in the external field (12) which give the coefficient functions in front of our Wilson-line operators U_i. Note that formally we obtained the source term with the gauge link ordered along the light-like line which is a potentially dangerous situation. Indeed, it is easy to see that already the first loop diagram shown in Fig. 7 is divergent. The reason is that the longitudinal integrals over α_p are unrestricted from below (if the Wilson line is light-like). However, this is not what we want for the coefficient functions because they should include only the integration over the region $\alpha_p > \sigma$ (the region $\alpha_p < \sigma$ belongs to matrix elements; see the discussion in Sec. III). Therefore, we must impose somehow this condition $\alpha_p > \sigma$ in our Feynman diagrams created by the source (17). Fortunately, we already faced a similar problem—how to impose a condition $\alpha_p < \sigma$ on the matrix elements of operators U (see Fig. 4) and we have solved that problem by changing the slope of the supporting line. We demonstrated that in order to cut the integration over large $\alpha > \sigma$ from matrix elements of Wilson-line operators U_i we need to change the slope of these Wilson-line operators to $n = \sigma p_1 + \tilde{\sigma} p_2$. Similarly, if we want to cut the integration over small $\alpha_p < \sigma$ from the coefficient functions we need to order the gauge factors in Eq. (17) along (the same) vector[3] $n = \sigma p_1 + \tilde{\sigma} p_2$.

Therefore, the final form of the generating functional for the Feynman diagrams (with $\alpha > \sigma$ cutoff) in the external field (13) is

$$\int \mathcal{D}\mathcal{A}\mathcal{D}\Psi \exp\left\{ iS(\mathcal{A}, \Psi) + i\int d^2 x_\perp U^{ai}(x_\perp) V_i^a(x_\perp) \right\}, \tag{29}$$

where

$$V_i(x_\perp) = \int_{-\infty}^{\infty} dv [-\infty n, vn]_{x_\perp} n^\mu F_{\mu i}(vn + x_\perp) [vn, -\infty n]_{x_\perp} \tag{30}$$

[3]Note that the diagram in Fig. 7 is the diagram in Fig. 4b turned upside down. In the Fig. 4b diagram we have a restriction $\alpha < \sigma$. It is easy to see that this also means a restriction $\beta > \tilde{\sigma}$ if one chooses to write down the rapidity integrals in terms of β's rather than α's. Turning the diagram upside down amounts to interchange of p_A and p_B which leads to (i) replacement of the slope of Wilson line by $\tilde{\sigma} p_1 + \sigma p_2$ and (ii) replacement $\alpha \leftrightarrow \beta$ in the integrals. Thus, the restriction $\beta > \tilde{\sigma}$ imposed by the line collinear to $\sigma p_1 + \tilde{\sigma} p_2$ in diagram in Fig. 4b means the restriction $\alpha > \tilde{\sigma}$ by the line collinear to $\tilde{\sigma} p_1 + \sigma p_2$ in the Fig. 7 diagram. After renaming σ by $\overline{\sigma}$ we obtain the desired result.

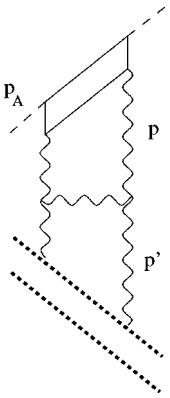

FIG. 7. A typical loop diagram in the external field created by the Wilson-line source (17).

and $V_i^a \equiv \mathrm{Tr}(\lambda^a V_i)$ as usual. For completeness, we have added integration over quark fields so $S(\mathcal{A},\Psi)$ is the full QCD action.

Now we can assemble the different parts of the factorization formula (4). We have written down the generating functional integral for the diagrams with $\alpha > \sigma$ in the external fields with $\alpha < \sigma$ and what remains now is to write down the integral over these ''external'' fields. Since this integral is completely independent of Eq. (29) we will use a different notation $\mathcal{B}$ and χ for the $\alpha < \sigma$ fields. We have:

$$\int \mathcal{D}A\mathcal{D}\bar{\Psi}\mathcal{D}\Psi e^{iS(A,\Psi)} j(p_A) j(p_A') j(p_B) j(p_B')$$
$$= \int \mathcal{D}\mathcal{A}\mathcal{D}\bar{\psi}\mathcal{D}\psi e^{iS(\mathcal{A},\psi)} j(p_A) j(p_A') \int \mathcal{D}\mathcal{B}\mathcal{D}\bar{\chi}\mathcal{D}\chi$$
$$\times j(p_B) j(p_B') e^{iS(\mathcal{B},\chi)} \exp\left\{ i \int d^2x_\perp U^{ai}(x_\perp) V_i^a(x_\perp) \right\}. \tag{31}$$

The operator U_i in an arbitrary gauge is given by the same formula (30) as operator V_i with the only difference that the gauge links and $F_{\cdot i}$ are constructed from the fields $\mathcal{B}_\mu$. This is our factorization formula (4) in the functional integral representation.

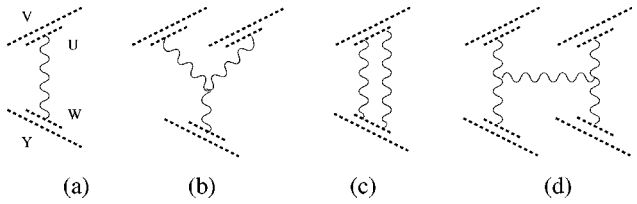

FIG. 8. Lowest order terms in the perturbative expansion of the effective action.

The functional integrals over $\mathcal{A}$ fields give logarithms of the type $g^2 \ln 1/\sigma$ while the integrals over slow $\mathcal{B}$ fields give powers of $g^2 \ln(\sigma s/m^2)$. With logarithmic accuracy, they add up to $g^2 \ln s/m^2$. However, there will be additional terms $\sim g^2$ due to mismatch coming from the region of integration near the dividing point $\alpha \sim \sigma$ where the details of the cutoff in the matrix elements of the operators U and V become important. Therefore, one should expect the corrections of order of g^2 to the effective action $\int dx_\perp U^i V_i$. Still, the fact that the fast quark moves along the straight line has nothing to do with perturbation theory (cf. Ref. [13]); therefore it is natural to expect the nonperturbative generalization of the factorization formula (31) constructed from the same Wilson-line operators U_i and V_i (probably with some kind of nonlocal interactions between them).

IV. EFFECTIVE ACTION FOR HIGH-ENERGY SCATTERING

The factorization formula gives us a starting point for a new approach to the analysis of the high-energy effective action. Consider another rapidity η_0' in the region between η_0 and $\eta_B = \ln m^2/s$. If we use the factorization formula (31) once more, this time dividing between the rapidities greater and smaller than η_0', we get the expression for the amplitude (6) in the form[4]

$$iA(s,t) = \int \mathcal{D}A e^{iS(A)} j(p_A) j(p_A') j(p_B) j(p_B')$$
$$= \int \mathcal{D}\mathcal{A} e^{iS(\mathcal{A})} j(p_A) j(p_A') \int \mathcal{D}\mathcal{B} e^{iS(\mathcal{B})} j(p_B) j(p_B') \int \mathcal{D}\mathcal{C} e^{iS(\mathcal{C})} e^{i\int d^2x_\perp V^{ai}(x_\perp) U_i^a(x_\perp) + i\int d^2x_\perp W^{ai}(x_\perp) Y_i^a(x_\perp)}. \tag{32}$$

In this formula the operators V_i (made from $\mathcal{A}$ fields) are given by Eq. (30), the operators U_i are also given by Eq. (30) but constructed from the $\mathcal{C}$ fields instead, and the operators W_i (made from $\mathcal{C}$ fields) and Y_i (made from $\mathcal{B}$ fields) are aligned along the direction $n' = \sigma' p_1 + \tilde{\sigma}' p_2$ corresponding to the rapidity η' (as usual, $\ln \sigma'/\tilde{\sigma}' = \eta'$ where $\tilde{\sigma}' = m^2/s\sigma'$):

$$U_i(\mathcal{C})_{x_\perp} = \int_{-\infty}^{\infty} dv [-\infty n, vn]_{x_\perp} n^\mu F_{\mu i}(vn + x_\perp) [vn, -\infty n]_{x_\perp},$$

[4]For brevity, we do not display the quark fields.

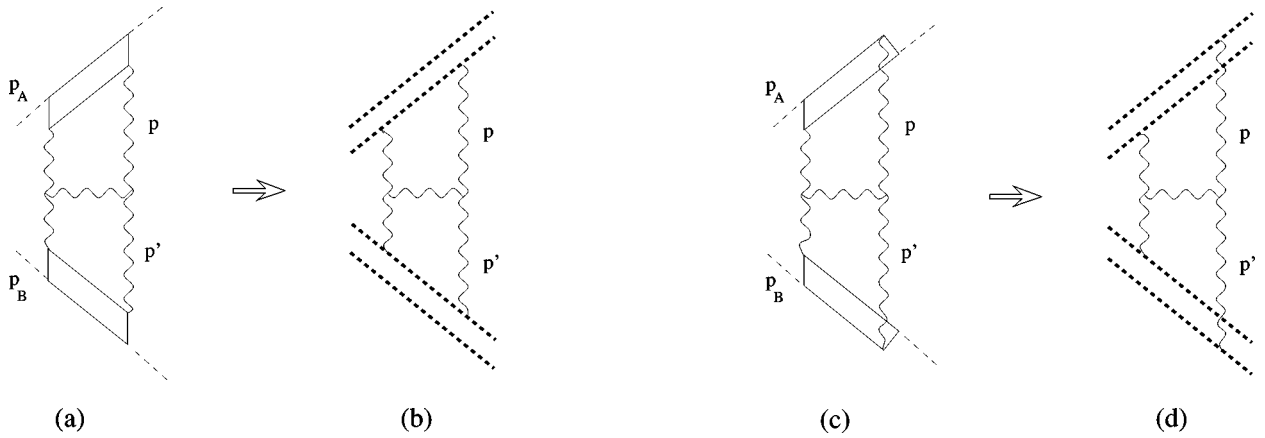

FIG. 9. Counting of loops for Feynman diagrams (a),(c) and the corresponding Wilson-line operators (b),(d).

$$W_i(\mathcal{C})_{x_\perp} = \int_{-\infty}^{\infty} dv\,[-\infty n', vn']_{x_\perp} n'^{\mu} F_{\mu i}(vn' + x_\perp)[vn', -\infty n']_{x_\perp},$$

$$Y_i(\mathcal{B})_{x_\perp} = \int_{-\infty}^{\infty} dv\,[-\infty n', vn']_{x_\perp} n'^{\mu} F_{\mu i}(vn' + x_\perp)[vn', -\infty n']_{x_\perp}.$$

Thus, we have factorized the functional integral over ''old'' $\mathcal{B}$ fields into the product of two integrals over $\mathcal{C}$ and ''new'' $\mathcal{B}$ fields.

Now, let us integrate over the $\mathcal{C}$ fields and write down the result in terms of an effective action. Formally, one obtains:

$$iA(s,t) = \int \mathcal{D}\mathcal{A} e^{iS(\mathcal{A})} j(p_A) j(p_A') \int \mathcal{D}\mathcal{B} e^{iS(\mathcal{B})} j(p_B) j(p_B') e^{iS_{\rm eff}(V_i, Y_i;\, \sigma/\sigma')} \tag{33}$$

where $S_{\rm eff}$ for the rapidity interval between η and η' is defined as

$$e^{iS_{\rm eff}(V_i, Y_i; \sigma/\sigma')} = \int \mathcal{D}\mathcal{C} e^{iS(\mathcal{C})} e^{i\int d^2x_\perp V^{ai}(x_\perp) U_i^a(x_\perp) + i\int d^2x_\perp W^{ai}(x_\perp) Y_i^a(x_\perp)}. \tag{34}$$

This formula gives a rigorous definition for the effective action for a given interval in rapidity (cf. Ref. [6]).

The next step would be to perform explicitly the integrations over the longitudinal momenta in the right-hand side (RHS) of Eq. (34) and obtain the answer for the integration over our rapidity region (from η to η') in terms of two-dimensional theory in the transverse coordinate space which hopefully would give us the unitarization of the BFKL Pomeron. At present, it is not known how to do this. One can obtain, however, the first few terms in the expansion of effective action in powers of V_i and Y_i. The easiest way to do this is to expand gauge factors U_i and W_i in RHS of Eq. (34) in powers of $\mathcal{C}$ fields and calculate the relevant perturbative diagrams (see Fig. 8). The first few terms in the effective action at the one-log level[5] have the form [3,18]:

[5]This ''one-log'' level corresponds to one-loop level for usual Feynman diagrams. Superficially, the diagram in Fig. 8d looks like the tree diagram in comparison to the diagram in Fig. 8c which has one loop. However, both of the diagrams in Figs. 8c and 8d contain integration over longitudinal momenta [and thus the factor $\ln(\sigma/\sigma')$] so in the longitudinal space the diagram in Fig. 8d is a loop diagram too. It happens because for diagrams with Wilson-line opertors the number of loops literally corresponds to the counting of the number of loop integrals only for the transverse momenta. For the longitudinal variables, the diagrams which look like trees may contain logarithmical loop integrations. This property is illustrated in Fig. 9: the Wilson-line diagrams shown in Fig. 9b has two loops and the diagram shown in Fig. 9d is a tree but both of them originated from Feynman diagrams shown in Figs. 9a and 9c with equal number of loops. To avoid confusion, we will use the term ''one-log level'' instead of ''one-loop level.''

$$S_{\rm eff}=\int d^2x V^{ai}(x)Y_i^a(x)-\frac{g^2}{64\pi^3}\ln\frac{\sigma}{\sigma'}\Bigg(N_c\int d^2xd^2yV^a_{i,i}(x)\ln^2(x-y)^2Y^a_{j,j}(y)$$

$$+\frac{f_{abc}f_{mnc}}{4\pi^2}\int d^2xd^2yd^2x'd^2y'd^2zV^a_{i,i}(x)V^m_{j,j}(y)Y^b_{k,k}(x')Y^n_{l,l}(y')$$

$$\times\ln\frac{(x-z)^2}{(x-x')^2}\ln\frac{(y-z)^2}{(y-y')^2}\left(\frac{\partial}{\partial z_i}\right)^2\ln\frac{(x'-z)^2}{(x-x')^2}\ln\frac{(y'-z)^2}{(y-y')^2}\Bigg)+\cdots, \tag{35}$$

where we use the notation $V^a_{i,j}(x)\equiv(\partial/\partial x_j)V^a_i(x)$, etc. The first term (see Fig. 8a) looks like the corresponding term in the factorization formula (31)—only the directions of the supporting lines are now strongly different.[6] The second term shown in Fig. 8c is the first-order expression for the Reggeization of the gluon [1] and the third term (see Fig. 8d) is the two-Reggeon Lipatov's Hamiltonian [14] responsible for BFKL logarithms.

Let us discuss subsequent terms in the perturbative expansion (35). There can be two types of the logarithmical contributions. First is the ''true'' loop contribution coming from the diagrams of the Fig. 10a type. This diagram is an iteration of the Lipatov's Hamiltonian. However, in the same $[\ln(\sigma/\sigma')]^2$ order there is another contribution coming from the diagram shown in Fig. 10a. To treat them separately, we can consider the case when $g\ll 1$ but the sources are strong $(\sim 1/g)$ so $gY_i\sim gU_i\sim 1$. In this case, the diagram in Fig. 10b has the order $g^4Y_i^2V_i^2[\ln(\sigma/\sigma')]^2\sim[\ln(\sigma/\sigma')]^2$ while the ''tree'' Fig. 8b diagram is

$$\sim g^4Y_i^3V_i^3[\ln(\sigma/\sigma')]^2\sim(1/g^2)[\ln(\sigma/\sigma')]^2.$$

So, in this approximation the tree diagrams are the most important and should be summed up in the first place. As usual, the best way to sum the tree diagrams is given by the semiclassical method which will be discussed in next section.

However, if we would like to get the result on the one-log level it can be obtained using the evolution equations for the Wilson-line operators [5]. Note that at this level we have only the diagrams of the Fig. 11 type. These diagrams describe the situation when one of the sources is weak and another is still strong (see also Refs. [15,16]). For example, if the source V_i is weak (and hence gV_i is a valid small parameter) but the source Y_i is not weak (so that $gV_i\sim 1$ is *not* a small parameter) one must take into account the diagrams shown in Figs. 11a and 11b. The multiple rescatterings in Figs. 11a,b describe the motion of the gluon emitted by the weak source V_i in the strong external field $A_i=Y_i\theta(x_*)$ created by the source Y_i. These diagrams were calculated in Ref. [5]. For example, the result of the calculation of the diagram in Fig. 11a presented in a form of the evolution of the Wilson-line operators U_i reads[7]

$$U^a_i(x_\perp)\to Y^a_i(x_\perp)-\frac{g^2}{8\pi^3}\ln\frac{\sigma}{\sigma'}\int dy_\perp\frac{1}{(x-y)^2_\perp}$$
$$\times(f^{abc}(Y^\dagger_x\partial_iY_y)^{bc}+N_cU^a_i(x_\perp))+\cdots, \tag{36}$$

where dots stand for the terms with extra $g^2\ln(\sigma/\sigma')$ factors. This evolution equation means that if we integrate over the rapidities $\eta_0>\eta>\eta_0'$ in the matrix elements of the operator U_i we will get the expression (36) constructed from the operators Y_i with rapidities up to η_0' times factors proportional to $g^2(\eta_0-\eta_0')\equiv g^2\ln(\sigma/\sigma')$. Therefore, the corresponding contribution to the effective action at the one-log level takes the form

$$\int dx_\perp V^a_i(x_\perp)U^{ai}(x_\perp)\to\int dx_\perp V^a_i(x_\perp)Y^{ai}(x_\perp)-\frac{g^2}{8\pi^3}\ln\frac{\sigma}{\sigma'}\int dx_\perp dy_\perp\frac{1}{(x-y)^2_\perp}[i(V^i(x_\perp)Y^\dagger_x\partial_iY_y)^{aa}-N_cV^{ai}(x_\perp)U^a_i(x_\perp)], \tag{37}$$

[6]Strictly speaking, the contribution coming from the diagram shown in Fig. 8a has the form $\int d^2xV^{ai}(x)(\partial_i\partial_j/\partial^2)Y^{aj}(x)$ which differs from the first term in RHS of Eq. (35) by $\int d^2xV^{ai}(x)(1/\partial^2)(\partial^2g_{ij}-\partial_i\partial_j)Y^{aj}(x)$. However, it may be demonstrated that this discrepancy [which is actually $\sim O(g)$ for a a pure gauge field Y_i] is canceled by the contribution from the diagram with three-gluon vertex shown in Fig. 8b just as in the case of perturbative calculation of $\mathcal{A}_i$ discussed in Sec. III.

[7]Here $Y_x\equiv Y(x_\perp)=[\infty n'+x_\perp,-\infty n'+x_\perp]$ so that $Y_i(x_\perp)=Y^\dagger_x i(\partial/\partial_i)Y_x$. [Note that we have the gauge factors in the gluon (adjoint) representation here.]

where the first term is the lowest-order effective action [$\equiv$ the first term in Eq. (35)] and the second term contains new information. To check this second term, we may expand it in powers of the source Y_i and it is easy to see that the first nontrivial term in this expansion coincides with the gluon-Reggeization term in Eq. (35).

Apart from the Eq. (37) term, there is another contribution to the one-loop evolution equations coming from the diagrams in Fig. 11b [5]:

$$U_i^a(x_\perp)U_j^b(y_\perp)\to-\frac{g^2}{4\pi^3}\ln\frac{\sigma}{\sigma'}\left(\nabla_i^x\left[\int dz_\perp\frac{(x-z)_\perp\cdot(y-z)_\perp}{(x-z)_\perp^2(y-z)_\perp^2}(Y_x^\dagger Y_y+1-Y_x^\dagger Y_z-Y_z^\dagger Y_y)\right]\tilde{\nabla}_j^y\right)^{ab} \tag{38}$$

where

$$\nabla_i^x\mathcal{O}(x_\perp)\equiv\frac{\partial}{\partial x^i}\mathcal{O}(x_\perp)-iU_i(x_\perp)\mathcal{O}(x_\perp),$$

$$\mathcal{O}(y_\perp)\tilde{\nabla}_i^y\equiv-\frac{\partial}{\partial y^i}\mathcal{O}(y_\perp)-i\mathcal{O}(y_\perp)U_i(y_\perp) \tag{39}$$

are the ''covariant derivatives'' (in the adjoint representation). The corresponding term in effective action has the form

$$\frac{ig^2}{8\pi^3}\ln\frac{\sigma}{\sigma'}\int dx_\perp dy_\perp(\nabla_i^xV_i^a)(x_\perp)\int dz_\perp\frac{(x-z)_\perp\cdot(y-z)_\perp}{(x-z)_\perp^2(y-z)_\perp^2}(Y_x^\dagger Y_y+1-Y_x^\dagger Y_z-Y_z^\dagger Y_y)^{ab}(\nabla_j^yV_j^b)(y_\perp). \tag{40}$$

The final form of the one-log effective action for this case is the sum of the expressions (37) and (40):

$$\begin{aligned}S_{\rm eff}^{(I)}(V_i,Y_j)=&\int d^2xV^{ai}(x)Y_i^a(x)-\frac{g^2}{8\pi^3}\ln\frac{\sigma}{\sigma'}\int dx_\perp dy_\perp\frac{1}{(x-y)_\perp^2}[i(V^i(x_\perp)Y_x^\dagger\partial_iY_y)^{aa}-N_cV^{ai}(x_\perp)U_i^a(x_\perp)]\\&+\frac{ig^2}{8\pi^3}\ln\frac{\sigma}{\sigma'}\int dx_\perp dy_\perp\nabla_i^xV^{ai}(x_\perp)\int dz_\perp\frac{(x-z)_\perp\cdot(y-z)_\perp}{(x-z)_\perp^2(y-z)_\perp^2}\\&\times(Y_x^\dagger Y_y+1-Y_x^\dagger Y_z-Y_z^\dagger Y_y)^{ab}\nabla_j^yV^{bj}(y_\perp),\end{aligned} \tag{41}$$

where V_i is a weak source and Y_i is a strong one. It is clear that if the source V_i is strong and Y_i is weak as shown in Fig. 10c,d diagrams the effective action $S_{\rm eff}^{(II)}(V_i,Y_j)$ will have the similar form with the replacement $V\leftrightarrow Y$.

As we mentioned above, the diagrams in Fig. 10 and Fig. 11 complete the list of diagrams which contribute to the effective action at the one-log level (even if both sources are strong). It means that the one-log answer in general case can be guessed by comparison of the answers for $S_{\rm eff}^{(I)}(V_i,Y_j)$ and $S_{\rm eff}^{(II)}(V_i,Y_j)$ (the simple sum is not enough since some of the contributions will be double-counted). Instead of doing that, we will obtain the one-log result for two strong sources using the semiclassical method and check that it agrees with Eq. (41).

V. EFFECTIVE ACTION AND COLLISION OF TWO SHOCK WAVES

The functional integral (34) which defines the effective action is the usual QCD functional integral with two sources corresponding to the two colliding shock waves. Instead of calculation of perturbative diagrams (as it was done in the previous section) one can use the semiclassical approach. This approach is relevant when the coupling constant is relatively small but the characteristic fields are large (in other words, when $g^2\ll1$ but $gV_i\sim gY_i\sim1$). In this case one can calculate the functional integral (34) by expansion around the new stationary point corresponding to the classical wave created by the collision of the shock waves.

With leading log accuracy, we can replace the vector n by p_1 and the vector n' by p_2. Then the functional integral (34) takes the form:

$$e^{iS_{\rm eff}(V_i,Y_i;\sigma/\sigma')}=\int\mathcal{D}Ae^{iS_{QCD}(A)}e^{i\int d^2x_\perp V^{ai}(x_\perp)U_i^a(x_\perp)+i\int d^2x_\perp W^{ai}Y_i^a(x_\perp)} \tag{42}$$

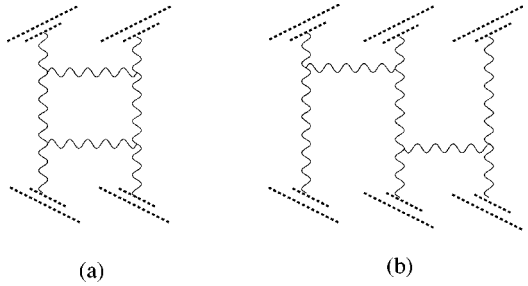

FIG. 10. Typical perturbative diagrams in the next $[\ln(\sigma/\sigma')]^2$ order.

where now

$$U_i^a(x_\perp)=\int_{-\infty}^{\infty} dv \hat{F}_{\bullet i}(vp_1+x_\perp),$$
$$W_i^a=\int_{-\infty}^{\infty} dv \tilde{F}_{*i}(vp_2+x_\perp). \tag{43}$$

Hereafter we use the notations

$$\hat{\mathcal{O}}(x)=[-\infty p_1+x,x]\mathcal{O}(x)[x,-\infty p_1+x],$$
$$\tilde{\mathcal{O}}(x)=[-\infty p_2+x,x]\mathcal{O}(x)[x,-\infty p_2+x]. \tag{44}$$

Note that we changed the name for the gluon fields in the integrand from $\mathcal{C}$ back to A.

As usual, the classical equation for the saddle point $\bar{A}$ in the functional integral (42) is

$$\frac{\delta}{\delta A}\left(S_{QCD}+\int d^2x_\perp V^{ai}(x_\perp)U_i^a(x_\perp) + \int d^2x_\perp W^{ai}Y_i^a(x_\perp)\right)\Big|_{A=\bar{A}}=0. \tag{45}$$

To write down them explicitly we need the first variational derivatives of the source terms with respect to gauge field. We have

$$\delta U_i=\delta\hat{A}_i(\infty p_1+x_\perp)-\delta A_i(-\infty p_1+x_\perp) - \int_{-\infty}^{\infty} du \hat{\nabla}_i \delta\hat{A}_i(up_1+x_\perp),$$
$$\delta W_i=\delta\tilde{A}_i(\infty p_2+x_\perp)-\delta A_i(-\infty p_2+x_\perp) - \int_{-\infty}^{\infty} du \tilde{\nabla}_i \delta\tilde{A}_i(up_2+x_\perp), \tag{46}$$

where

$$\hat{\nabla}_i\mathcal{O}(x)\equiv\partial_i\mathcal{O}(x)-i[U_i(x_\perp)+A_i(-\infty p_1+x_\perp),\mathcal{O}(x)],$$

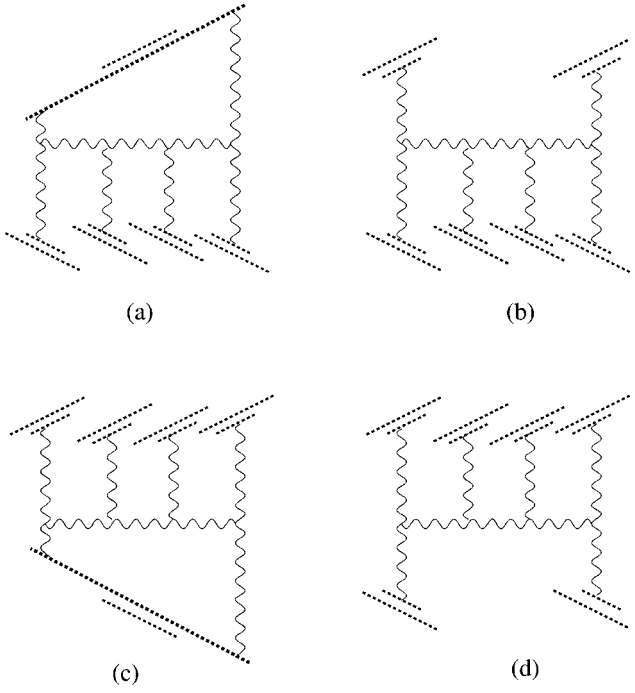

FIG. 11. Perturbative diagrams for the effective action in the case of one weak source and one strong one.

$$\tilde{\nabla}_i\mathcal{O}(x)\equiv\partial_i\mathcal{O}(x)-i[W_i(x_\perp)+A_i(-\infty p_2+x_\perp),\mathcal{O}(x)]. \tag{47}$$

Therefore the explicit form of the classical equations (45) for the wave created by the collision is

$$D^\mu F_{\mu i}=0,$$
$$D^\mu F_{*\mu}=\delta\left(\frac{2}{s}x_\bullet\right)\left[\frac{2}{s}x_* p_1,-\infty p_1\right]_{x_\perp} \times\hat{\nabla}_i V^i(x_\perp)\left[-\infty p_1,\frac{2}{s}x_* p_1\right]_{x_\perp},$$
$$D^\mu F_{\bullet\mu}=\delta\left(\frac{2}{s}x_*\right)\left[\frac{2}{s}x_\bullet p_2,-\infty p_2\right]_{x_\perp} \times\tilde{\nabla}_i Y^i(x_\perp)\left[-\infty p_2,\frac{2}{s}x_\bullet p_2\right]_{x_\perp}. \tag{48}$$

These equations define the classical field created by the collision of two shock waves.[8] Unfortunately, it is not clear

[8]They are essentially equivalent to the classical equations describing the collision of two heavy nuclei in Ref. [16].

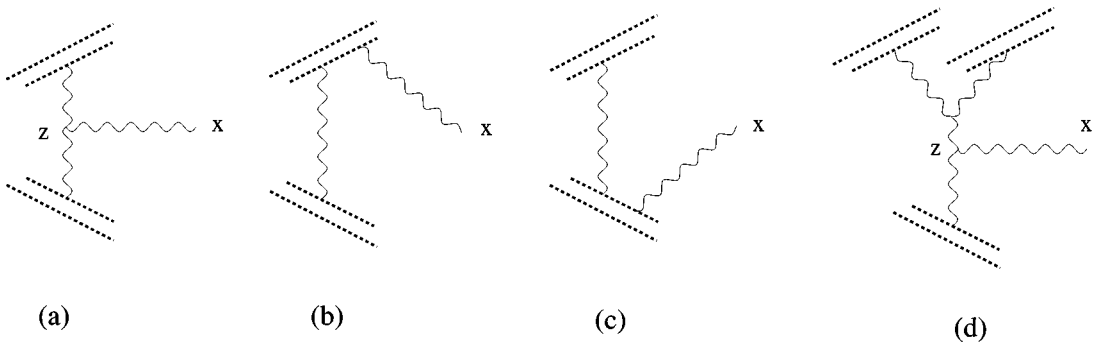

FIG. 12. Perturbative Feynman diagrams for the field strength (51).

how to solve these equations. One can start with the trial field which is a simple superposition of the two shock waves (12)

$$A_*^{(0)}=A_\bullet^{(0)}=0, \quad A_i^{(0)}=\Theta(x_\bullet)V_i+\Theta(x_*)Y_i \tag{49}$$

and improve it by taking into account the interaction between the shock waves order by order [17]. The parameter of this expansion is the commutator $g^2[Y_i,V_k]$. Moreover, it can be demonstrated that each extra commutator brings a factor $\ln(\sigma/\sigma')$ and therefore this approach is a sort of leading logarithmic approximation. In the lowest nontrivial order one gets

$$A_i^{(1)}=-\frac{g}{4\pi^2}\int dz_\perp([Y_i(z_\perp),V_k(z_\perp)]-i\leftrightarrow k)\frac{(x-z)^k}{(x-z)_\perp^2}$$
$$\times\left\{\ln\left(1-\frac{(x-z)_\perp^2}{x_\parallel^2+i\epsilon}\right)+2\pi i\,\theta(x_*)\,\theta(x_\bullet)\right\}, \tag{50}$$

$$A_\bullet^{(1)}=\frac{gs}{16\pi^2}\int dz_\perp\frac{1}{x_*+i\epsilon}\ln(-x_\parallel^2+(x-z)_\perp^2+i\epsilon)$$
$$\times[Y_k(z_\perp),V^k(z_\perp)],$$

$$A_*^{(1)}=-\frac{gs}{16\pi^2}\int dz_\perp\frac{1}{x_\bullet+i\epsilon}\ln(-x_\parallel^2+(x-z)_\perp^2+i\epsilon)$$
$$\times[Y_k(z_\perp),V^k(z_\perp)],$$

where $x_\parallel^2\equiv(4/s)x_*x_\bullet$ is a longitudinal part of x^2. These fields are obtained in the background-Feynman gauge. The corresponding expressions for field strength have the form

$$F_{\bullet *}^{(1)}=\frac{gs}{4\pi^2}\int dz_\perp\frac{1}{-x_\parallel^2+(x-z)_\perp^2+i\epsilon}[Y_k,V^k],$$

$$F_{ik}^{(1)}=\frac{g}{2\pi^2}\int dz_\perp\frac{1}{-x_\parallel^2+(x-z)_\perp^2+i\epsilon}$$
$$\times([Y_i,V_k]-[Y_k,V_i]),$$

$$F_{\bullet i}^{(1)}=\frac{gs}{8\pi^2}\int dz_\perp\frac{(x-z)^k}{-x_\parallel^2+(x-z)_\perp^2+i\epsilon}$$
$$\times\left(\frac{g_{ik}[Y_j,V^j]}{x_*-i\epsilon}+\frac{[Y_i,V_k]-[Y_k,V_i]}{x_*+i\epsilon}\right),$$

$$F_{*i}^{(1)}=-\frac{gs}{8\pi^2}\int dz_\perp\frac{(x-z)^k}{-x_\parallel^2+(x-z)_\perp^2+i\epsilon}$$
$$\times\left(\frac{g_{ik}[Y_j,V^j]}{x_\bullet-i\epsilon}-\frac{[Y_i,V_k]-[Y_k,V_i]}{x_\bullet+i\epsilon}\right). \tag{51}$$

In terms of usual Feynman diagrams (when we expand in powers of source just like in the previous section) these expressions come from the diagrams shown in Fig. 12. When we sum up the three contributions from the diagrams in Figs. 12a,b, and c the three-gluon vertex in Fig. 12a is replaced by the effective Lipatov's vertex and we get Eq. (51) up to the terms $(1/\partial^2)\partial_i\partial_kY^k$ and $(1/\partial^2)\partial_j\partial_kV^k$ standing in place of Y_i and V_j. However, as we have discussed in Sec. III, the difference $Y_i-(1/\partial^2)\partial_i\partial_kY^k=g(\partial_k/\partial^2)[Y_i,Y_k]$ (which has an additional power of g) will be canceled by the next-order perturbative diagrams of the Fig. 12d type.

Let us now find the effective action. In the trivial order the only nonzero field strength components are $F_{\bullet i}^{(0)}=\delta[(2/s)x_*]Y_i(x_\perp)$ and $F_{*i}^{(0)}=\delta[(2/s)x_\bullet]V_i(x_\perp)$ so we get the familiar expression $S^{(0)}=\int d^2x_\perp V^{ai}Y_i^a$. In the next order one has

$$S^{(1)}=\int d^4x\left(-\frac{2}{s}F_*^{(1)ai}F_{\cdot i}^{(1)a}-\frac{1}{4}F_{ik}^{(1)a}F^{(1)aik}+\frac{2}{s^2}F_{*\cdot}^{(1)a}F_{*\cdot}^{(1)a}\right)$$

$$+2\int d^2x_\perp\int du[\mathrm{Tr}V^i([-\infty p_1,up_1]_{x_\perp}F_{\cdot i}(up_1+x_\perp)[up_1+x_\perp,-\infty p_1]_{x_\perp})^{(1)}$$

$$+\mathrm{Tr}Y^i([-\infty p_2,up_2]_{x_\perp}F_{*i}(up_2+x_\perp)[up_2,\infty p_2]_{x_\perp})^{(1)}]. \tag{52}$$

We have seen above that the effective action contains $\ln(\sigma/\sigma')$ [see Eq. (35)]. With logarithmic accuracy, the RHS of Eq. (52) reduces to

$$S^{(1)}=-\frac{2}{s}\int d^4xF_*^{(1)ai}(x)F_{\cdot i}^{(1)a}(x)$$

$$+\int d^2x_\perp 2\mathrm{Tr}[Y^i,V_i]([x_\perp,-\infty p_2+x_\perp]^{(1)}$$

$$-[x_\perp,-\infty p_1+x_\perp]^{(1)}). \tag{53}$$

The first term contains the integral over $d^4x=(2/s)dx_\cdot dx_* d^2x_\perp$. In order to separate the longitudinal divergencies from the infrared divergencies in the transverse space we will work in the $d=2+2\epsilon$ transverse dimensions. It is convenient to perform at first the integral over x_* which is determined by a residue in the point $x_*=0$. The integration over the remaining light-cone variable $x_\cdot$ factorizes then in the form $\int_0^\infty dx_\cdot/x_\cdot$ or $\int_{-\infty}^0 dx_\cdot/x_\cdot$. This integral reflects our usual longitudinal logarithmic divergencies which arise from the replacement of vectors n and n' in Eq. (34) by the light-like vectors p_1 and p_2. In the momentum space this logarithmical divergency has the form $\int d\alpha/\alpha$. It is clear that when α is close to σ (or σ') we can no longer approximate n by p_1 (or n' by p_2). Therefore, in the leading log approximation this divergency should be replaced by $\ln(\sigma/\sigma')$:

$$\int_0^\infty dx_\cdot\frac{1}{x_\cdot}=\int_0^\infty d\alpha\frac{1}{\alpha}\to\int_\sigma^{\sigma'}d\alpha\frac{1}{\alpha}=\ln\frac{\sigma}{\sigma'}. \tag{54}$$

The (first-order) gauge links in the second term in the RHS of Eq. (53) have the logarithmic divergence of the same origin:

$$[x_\perp,-\infty p_1+x_\perp]^{(1)}=-\frac{i}{8\pi^2}\int_{-\infty}^0\frac{dx_*}{x_*}\int d^2x_\perp\frac{\Gamma(\epsilon)}{(x-z)_\perp^{2\epsilon}}[Y_k(z_\perp),V^k(z_\perp)],$$

$$[x_\perp,-\infty p_2+x_\perp]^{(1)}=\frac{i}{8\pi^2}\int_{-\infty}^0\frac{dx_\cdot}{x_\cdot}\int d^2x_\perp\frac{\Gamma(\epsilon)}{(x-z)_\perp^{2\epsilon}}[Y_k(z_\perp),V^k(z_\perp)], \tag{55}$$

which also should be replaced by $\ln(\sigma/\sigma')$. Performing the remaining integration over $x_\perp$ in the first term in the RHS of Eq. (53) we obtain the the first-order classical action in the form

$$S^{(1)}=-\frac{ig^2}{8\pi^2}\ln\frac{\sigma}{\sigma'}\int d^2x_\perp d^2y_\perp(L_1^a(x_\perp)L_1^a(y_\perp)$$

$$+L_2^a(x_\perp)L_2^a(y_\perp))\frac{\Gamma(\epsilon)}{(x-y)_\perp^{2\epsilon}}, \tag{56}$$

where

$$L_1^a=if^{abc}Y_j^aV^{bj},\quad L_2^a=i\epsilon_{ik}Y^{ai}V^{bk}, \tag{57}$$

and ϵ_{ik} is the totally antisymmetric tensor in two transverse dimensions ($\epsilon_{12}=1$). One may also rewrite this expression in a compact form

$$S^{(1)}=\frac{ig^2}{2\pi}\ln\frac{\sigma}{\sigma'}\int d^2x_\perp\left(L_1^a\frac{1}{\partial_\perp^2}L_1^a+L_2^a\frac{1}{\partial_\perp^2}L_2^a\right). \tag{58}$$

A more accurate version of this formula looks like

$$S^{(1)}=\frac{ig^2}{2\pi}\ln\frac{\sigma}{\sigma'}\int d^2x_\perp\Bigg[L_1^a\frac{1}{\partial_\perp^2}L_1^a+L_2^a\left(Y^\dagger\frac{1}{\partial_\perp^2}Y+V^\dagger\frac{1}{\partial_\perp^2}V-\frac{1}{\partial_\perp^2}\right)^{ab}L_2^b$$

$$+L_1^a\left(\frac{\partial_i}{\partial^2}Y^\dagger\frac{\partial_k}{\partial^2}Y-Y\leftrightarrow V\right)L_2^b\epsilon^{ik}-L_2^a\epsilon^{ik}\left(Y^\dagger\frac{\partial_i}{\partial^2}Y\frac{\partial_k}{\partial^2}-Y\leftrightarrow V\right)^{ab}L_1^b\Bigg]+O([Y,V]^3), \tag{59}$$

where

$$Y(x_\perp)=[\infty p_1,-\infty p_1]_{x_\perp},\quad V(x_\perp)=[\infty p_2,-\infty p_2]_{x_\perp}. \tag{60}$$

It is easy to see that in the case of one weak and one strong source this expressions coincides with Eq. (40) (up to the terms of higher order in weak source which we neglect anyway).

At $d=2$ we have an infrared pole in $S^{(1)}$ which must be canceled by the corresponding divergency in the trajectory of the Reggeized gluon. The gluon Reggeization is not a classical effect in our approach—rather, it is a quantum correction coming from the loop corresponding to the determinant of the operator of second derivative of the action

$$\frac{\delta}{\delta A_\mu}\frac{\delta}{\delta A_\nu}\left(S_{QCD}+\int d^2x_\perp V^{ai}(x_\perp)U_i^a(x_\perp)+\int d^2x_\perp W^{ai}Y_i^a(x_\perp)\right)\Bigg|_{A=\bar{A}}. \tag{61}$$

The lowest-order diagrams are shown in Fig. 13 and the explicit form of the second derivative of the Wilson-line operator is

$$\delta U_i=i\int_{-\infty}^{\infty}du\int_{-\infty}^{u}dv[\delta\hat{A}_i(up_1+x_\perp),\hat{\nabla}_i\delta\hat{A}_i(vp_1+x_\perp)],$$

$$\delta W_i=i\int_{-\infty}^{\infty}du\int_{-\infty}^{u}dv[\tilde{A}_i(up_2+x_\perp),\tilde{\nabla}_i\delta\tilde{A}_i(up_2+x_\perp)]. \tag{62}$$

Now one easily gets the contribution of the Fig. 13 diagrams in the form

$$S_{\rm r}=\frac{g^2N_c}{8\pi^3}\ln\frac{\sigma}{\sigma'}\int d^2x_\perp d^2y_\perp[V_i^a(x_\perp)Y^{ai}(y_\perp)-V_i^a(x_\perp)Y^{ai}(x_\perp)]\frac{\Gamma^2(1+\epsilon)}{[(x-y)_\perp^2]^{(1+2\epsilon)}}. \tag{63}$$

A more accurate form of this equation reads

$$S_{\rm r}=-\frac{g^2N_c}{8\pi^3}\ln\frac{\sigma}{\sigma'}\int d^2x_\perp d^2y_\perp\frac{\Gamma^2(1+\epsilon)}{[(x-y)_\perp^2]^{(1+2\epsilon)}}\times\left\{V_i^a(x_\perp)Y^{ai}(x_\perp)-\frac{1}{N_c}(Y^i(x_\perp)\{Y(x_\perp)Y^\dagger(y_\perp)+V(x_\perp)V^\dagger(y_\perp)-1\}Y^i(y_\perp))^{aa}\right\}+O([Y,V]), \tag{64}$$

where $\mathcal{O}^{aa}\equiv\mathrm{Tr}\,O$ in the gluonic representation. In the case of one strong and one weak source it coincides with Eq. (37) (up to the higher powers of weak source).

The complete first-order ($\equiv$ one-log) expression for the effective action is the sum of $S^{(0)}$, $S^{(1)}$, and $S_{\rm r}$:

$$S_{\rm eff}=\int d^2xV^{ai}(x)Y_i^a(x)-\frac{ig^2}{8\pi^2}\ln\frac{\sigma}{\sigma'}\int d^2xd^2y\Bigg\{\frac{\Gamma(\epsilon)}{(x-z)^{2\epsilon}}[L_1^a(x)L_1^a(y)+L_2^a(x)L_2^b(y)(Y_x^\dagger Y_y+V_x^\dagger V_y-1)^{ab}]$$

$$\times\int d^2z\frac{\epsilon^{ij}(x-z)_i(z-y)_j}{\pi^2(x-z)^2(z-y)^2}[L_1^a(x)(Y_z^\dagger Y_y-Y\leftrightarrow V)^{ab}L_2^b(y)-L_2^a(x)(Y_x^\dagger Y_z-Y\leftrightarrow V)^{ab}L_1^b(y)]\Bigg\}$$

$$-\frac{g^2N_c}{8\pi^3}\ln\frac{\sigma}{\sigma'}\int d^2x_\perp d^2y_\perp\frac{\Gamma^2(1+\epsilon)}{[(x-y)_\perp^2]^{(1+2\epsilon)}}\Bigg\{V_i^a(x_\perp)Y^{ai}(x_\perp)-\frac{1}{N_c}[V^i(x_\perp)\{Y(x_\perp)Y^\dagger(y_\perp)$$

$$+V(x_\perp)V^\dagger(y_\perp)-1\}Y^i(y_\perp)]^{aa}\Bigg\}. \tag{65}$$

At one weak and one large source it coincides with Eq. (41). [As we discussed in Sec. IV, the new nontrivial terms in the case of two strong sources start from $[Y,V]^3\ln^2(\sigma/\sigma')$.]

As usual, in the case of scattering of white objects the logarithmic infrared divergence $\sim 1/\epsilon$ cancels. For example, for the case of one-Pomeron exchange the relevant term in the expansion of $e^{iS_{\rm eff}}$ has the form

$$-\frac{g^2}{16\pi^2}\ln\frac{\sigma}{\sigma'}\int d^2x_\perp d^2y_\perp f^{dam}(V_j^a Y^{mj} g_{ik}+V_i^a Y_k^m - V_k^a Y_i^m)(x_\perp)\frac{\Gamma(\epsilon)}{(x-y)_\perp^{2\epsilon}} f^{dbn}(V_l^b Y^{nl} g^{ik}+V^{bi}Y^{mk}-V^{bk}Y^{mi})(y_\perp)$$

$$+\frac{g^2 N_c}{16\pi^3}\ln\frac{\sigma}{\sigma'}\int d^2x_\perp V_i^a(x_\perp)Y^{ai}(x_\perp)\int d^2y_\perp d^2y'_\perp [V_j^b(y_\perp)-V_j^b(y'_\perp)]\frac{\Gamma^2(1+\epsilon)}{[(y-y')_\perp^2]^{(1+2\epsilon)}}[Y^{bj}(y_\perp)-Y^{bj}(y'_\perp)]. \quad (66)$$

It is easy to see that the terms $\sim 1/\epsilon$ cancel if we project onto colorless state in t-channel [that is, replace $V^{ai}V_j^b$ by $[\delta_{ab}/(N_c^2-1)]V^{ci}V_j^c$]. It is worth noting that in the two-gluon approximation the RHS of Eq. (66) gives the BFKL kernel.

VI. CONCLUSIONS AND OUTLOOK

First I would like to discuss the relation of this method to other approaches to the high-energy effective action discussed in the literature.

Historically, the idea how to reduce QCD at high energies to the two-dimensional effective theory was first suggested in Ref. [3] where the leading term in Eq. (35) was obtained. However, careful analysis of the assumptions made in this paper shows that the authors considered the fixed-angle limit of the theory ($s,t\to\infty$) rather than the Regge limit (where $\to\infty$ but t is fixed). It turns out that the first term in Eq. (35) is the same for both limits, but the subsequent terms differ.

Careful analysis of the effective action in the Regge limit was performed in the papers by Lipatov and collaborators [18]. The definition of the effective action in these papers is close to Eq. (33). However, the effective action is presented there in terms of the Reggeons built from fast and slow gluons rather than from the corresponding Wilson-line operators V_i and Y_i. In the first order, when the Reggeized gluon is identical to the usual gluon the expressions for the effective action are equivalent. In general, the explicit formula for the relation of the Reggeized gluons to usual gluon operators is not known and therefore it is not possible to compare the intermediate formulas for the higher terms in the effective action. Hoewever, since the physical results for the BFKL Pomeron and the three-Pomeron vertex coincide I think that the effective action obtained in Refs. [18,6] is equivalent to Eq. (33).

The most close in spirit to our semiclassical method is the renormalization-group approach to the high-energy scattering from the large nuclei advocated in the papers of McLerran and collaborators (see, e.g., Refs. [15,8,19]). In this approach, the small-x evolution of one strong shock wave is studied in the light-like gauge. (With such choice of gauge the second shock wave can be treated perturbatively at the very end of the evolution process.) The strong shock wave is created by the sources $\rho(x_\perp)$ so the evolution of the effective action $S(\rho)$ is obtained. In our terms, this amounts to the solution of classical Eqs. (48) using the trial configuration $A_i=U_i\theta(x_*)$ [instead of starting point $A_i=U_i\theta(x_*)+V_i\theta(x_*)$ taken in this paper]. Unfortunately, due to different gauges adopted in our paper and Refs. [8,19] the treatment of the boundary terms in the functional integral is different which leads to the different sources for the shock waves and makes it hard to compare the intermediate formulas. However, since again the BFKL results coincide I think these effective actions are essentially the same.

Also, there is a paper [20] where the notion of the effective action for the given interval in rapidity is discussed in terms very close to the present paper. The general idea is the same (as in this paper or in the approaches mentioned above). Unfortunately, the authors have not reproduced the BFKL Pomeron so it is difficult to compare the expressions for the effective action.

In conclusion I would like to outline possible uses of this approach. The ultimate goal is to obtain the explicit expression for the effective action in all orders in $\ln(s/m^2)$. One possible prospect is that due to the conformal invariance of QCD at the tree level our future result for the effective action can be formalized in terms of conformal two-dimensional theory in external two-dimensional ''gauge fields'' V_i and Y_i. So far, I was not able to use the conformal invariance because it is not obvious how to implement it in terms of Wilson-line operators. We can, however, expand Wilson lines back to gluons. The conformal properties of (Reggeized) gluon amplitudes are well studied now. In the coordinate space the BFKL kernel is invariant under Mobius group and therefore the eigenfunctions of the BFKL kernel are simply powers of coordinates. Moreover, at large N_c the diagrams with fixed number of Reggeized gluons (which form a *unitary* subset of all diagrams) may be described in terms of two-dimensional quantum mechanics of the particles with Lipatov's Hamiltonian ([14]). Due to the property

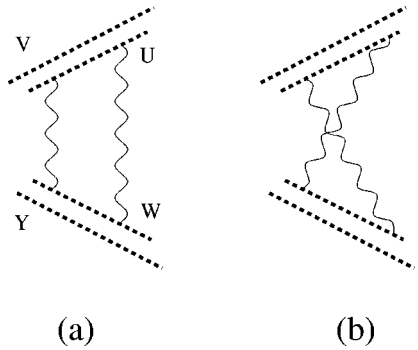

FIG. 13. Lowest-order diagrams for gluon Reggeization.

of a holomorphic separability this two-dimensional quantum mechanics reduces to the one-dimensional Heisenberg xxx spin-0 model [21]. (Unfortunately, the exact solution of this model is not known yet.) It is not clear which part of this symmetry survives for the full effective action but there is every reason to believe that it will simplify the structure of the answer even after reassembling of Wilson lines.

The semiclassical approach developed above for the small-x processes in perturbative QCD can be applied for studying the heavy-ion collisions. As advocated in Ref. [15], for the heavy-ion collisions the coupling constant may be relatively small due to high density. On the other hand, the fields produced by colliding ions are large so that the product gA is not small—which means that the Wilson-line gauge factors V and Y are of order of 1. It should be mentioned, however, that in this paper we considered the special case of the collision of the two shock waves, namely without any particles in the final state. It follows from the usual boundary conditions for Feynman amplitude (8) which we calculate: no outgoing waves at $t\to\infty$ (and no incoming fields at $t\to -\infty$, but we have satisfied this condition by choosing the gauge $A|_{t\to-\infty}=0$). However, people are usually interested in the process of particle production during the collision (see e.g. [22]) since it gives the experimental probe of quark-gluon plasma. In this case, our approach must be modified for the new boundary conditions—we must solve the classical equations (48) with Feynman boundary conditions only at $t\to-\infty$. The boundary condition at $t\to\infty$ depends on the problem under investigation: in case we are interested in the total cross section (cut diagrams) we must calculate the double functional integral corresponding to the integration over the ''+'' fields to the right and the ''−'' fields to the left of the cut (see Ref. [23]). (This is actually a functional-integral formalization of Cutkovsky rules.) In this case we may use the usual (Feynman and c.c. Feynman) propagators for each type of the fields. The boundary condition requires that two types of the field — the left-side ''−'' fields and the right-side ''+'' ones — coincide at $t\to\infty$. [This boundary condition is responsible for the $\delta(p^2)\theta(p_0)$ propagators on the cut.] Thus, to find the total cross section of the shock-wave collision in the semiclassical approximation we must solve the double set of classical equations for ''+'' and ''−'' fields with the boundary condition that these fields coincide at infinity. The study is in progress.

ACKNOWLEDGMENTS

The author is grateful to Y. Kovchegov, L. N. Lipatov, L. McLerran, and A. V. Radyushkin for valuable discussions. This work was supported by the U.S. Department of Energy under contract DE-AC05-84ER40150.

[1] V. S. Fadin, E. A. Kuraev, and L. N. Lipatov, Phys. Lett. **60B**, 50 (1975); I. I. Balitsky and L. N. Lipatov, Yad. Fiz. **28**, 439 (1978) [Sov. J. Nucl. Phys. **28**, 822 (1978)].
[2] V. S. Fadin and L. N. Lipatov, Phys. Lett. B **429**, 127 (1998).
[3] H. Verlinde and E. Verlinde, ''QCD at High Energies and Two-Dimensional Field Theory,'' Report No. PUPT-1319, e-print Archive: hep-th/9302104.
[4] J. C. Collins, D. R. Soper, and G. Sterman, in *Perturbative QCD*, edited by A. H. Mueller (World Scientific, Singapore, 1989).
[5] I. Balitsky, Nucl. Phys. **B463**, 99 (1996).
[6] L. N. Lipatov, Phys. Rep. **286**, 131 (1997).
[7] I. Balitsky, Phys. Rev. Lett. **81**, 2024 (1998).
[8] L. McLerran and R. Venugopalan, Phys. Rev. D **50**, 2225 (1994); A. Ayala, J. Jalilian-Marian, L. McLerran, and R. Venugopalan, *ibid.* **52**, 2935 (1995).
[9] O. Nachtmann, Ann. Phys. (N.Y.) **209**, 436 (1991).
[10] I. I. Balitsky and L. N. Lipatov, Pis'ma Zh. Éksp. Teor. Fiz. **30**, 383 (1979) [JETP Lett. **30**, 355 (1979)].
[11] I. Balitsky and V. M. Braun, Nucl. Phys. **B311**, 541 (1989).
[12] I. I. Balitsky, Nucl. Phys. **B254**, 166 (1985).
[13] H. G. Dosch, E. Ferreira, and A. Kraemer, Phys. Rev. D **50**, 1992 (1994).
[14] L. N. Lipatov, Zh. Éksp. Teor. Fiz. **90**, 1536 (1986) [Sov. Phys. JETP **63**, 904 (1986)].
[15] L. McLerran and R. Venugopalan, Phys. Rev. D **49**, 2233 (1994); **49**, 3352 (1994).
[16] A. Kovner, L. McLerran, and H. Weigert, Phys. Rev. D **52**, 6231 (1995).
[17] I. Balitsky, *Continuous Advances in QCD 98* (World Scientific, Singapore, 1998), e-print archive: hep-ph/9808215.
[18] R. Kirschner, L. N. Lipatov, and L. Szymanowski, Nucl. Phys. **B425**, 579 (1994); L. N. Lipatov, *ibid.* **B452**, 369 (1996).
[19] J. Jalilian-Marian, A. Kovner, and H. Weigert, Phys. Rev. D **59**, 014015 (1999).
[20] V. Kim and G. Pivovarov, Phys. Rev. Lett. **79**, 809 (1997).
[21] L. N. Lipatov, Pis'ma Zh. Éksp. Teor. Fiz. **59**, 571 (1994) [JETP Lett. **59**, 596 (1994)]; L. D. Faddeev and G. P. Korchemsky, Phys. Lett. B **342**, 311 (1995).
[22] Yu. V. Kovchegov and A. H. Mueller, Nucl. Phys. **B529**, 451 (1998).
[23] I. Balitsky and V. M. Braun, Nucl. Phys. **B361**, 93 (1991); **B380**, 51 (1992).